Receive Signal Strength Tumor Localization Using Magnetic Nanoparticles and SQUIDs

Hooman Lal Dehghani[*1], Kamal Shadi[2], okhtay Jahanbakhsh[3]

Department of Engineering and Emerging Technologies, University of Tabriz, Tabriz, Iran

[*1]h.Ldehghani88@ms.tabrizu.ac.ir; [2]kamalshadi@ece.gatech.edu; [3]o.jahanbakhsh@tabrizu.ac.ir

Abstract

In this paper we have modeled magnetic nanoparticle mathematically and have utilized a semi-classical approach based on Landau–Lifshitz Gilbert (LLG) equations. Our approach has based on Finite Element Method (FEM) as a numerical technique for finding approximate solutions of partial differential equations (PDE). The solution approach is based either on steady state problems, or rendering the PDE into an approximating system of ordinary differential equations, which are then numerically integrated using standard techniques. The proposed model has applied to three kind of magnetic nanoparticles including FluidMAG-DXS, FluidMAG-CMX and FluidMAG-PEI. Then Received Signal Strength (RSS) localization is utilized to find the true location of tumor where nanoparticles attached to it. The results of simulation prove that the error location can be less than 0.1 Cm. Researchers and clinicians can take advantage of these results in order for nanotechnology to make an impact in the diagnosis and treatment of malignancy. Furthermore the proposed model for magnetic nanoparticles can be used in improvement of drug delivery, cancer detection, diagnosis, imaging, and therapy while reducing toxicity.

Keywords

Nanoparticles; Landau–Lifshitz Gilbert; Received Signal Strength Localization; Bloch equation; Finite Element Method; Partial Differential Equations; Delaunay Algorithm; Galerkin Method

Introduction

Cancer is a major cause of death throughout the world, accounts for nearly one-quarter of total human mortality. Cancers treatment at an early stage of development allowing complete surgical removal is the most effective cancer therapy. Thus better method for detecting tumor at an early stage with low cost, noninvasive and precise techniques are the topic of extensive ongoing search and still is not fully achieved [1]. To this date, there are many imaging techniques that have been developed for cancer diagnosis, such as x-ray Computed Tomography (CT), Magnetic Resonance Imaging (MRI), and Positron Emission Tomography (PET). Although these imaging techniques are highly effective and widely utilized, they are expensive and their data interpretation is time-consuming. Furthermore in the cases that the patient is not allowed to expose in strong magnetic field, some of traditional approaches are not more practical.

Cancer nanotechnology has the potential to significantly enhance current techniques to cancer detection, drug delivery, diagnosis, imaging, and therapy while reducing toxicity associated with traditional cancer therapy [2-3]. A wide variety of nanomaterials are currently under investigation and development for application relative to cancer nanotechnology including; polymers, dendrimers, lipids, organometallic, carbon based materials and magnetic nanoparticles [4-6]. In this case a variety of nanoscale magnetic Resonance Imaging (MR) contrast agents have been developed [7]. These particles have received significant attention, given the widespread use of MR in clinical practice currently [8].

In nanotechnology cancer treatment, one of the most hopeful techniques is the use of magnetic nanoparticles. Magnetic nanoparticles have diameters ranging from several nanometers to several hundred nanometers (nm). They also possess special properties useful in the design of new cancer detection systems [9]. Living cells are typically 10 μm in diameter and include of many smaller components like endoplasmic reticulum, mitochondrion and nucleus. Proteins are even smaller with a typical size of just 5 nm, which is comparable to the dimensions of the current smallest man-made nanoparticles [10]. The comparable size of nanoparticles and biological building blocks suggests the possibility of using nanoparticles as probes to spy on the working of intracellular machinery without introducing much interference [10]. Recently scientists have found that magnetic nanoparticles can be especially helpful in locating cancerous cell clusters during MRI scans. Like teeny guide missiles, the nanoparticles seek out tumor cells and attach

themselves to them. Once the nanoparticles bind themselves to these cancer cells, the particles operate like radio transmitters, greatly aiding the MRI's detection capability. Advancement in molecular biology is increasing understanding of rationale and relevant molecular targets in cancer. However, due to the heterogeneity of the molecular abnormalities in multiple tumor types, strategies designed to interfere with multiple molecular abnormalities will be necessary to impact survival. Nanoparticles have the potential to provide therapies not possible with other drug modalities. Researchers and clinicians must take advantage of these opportunities in order for nanotechnology to make an impact in the diagnosis and treatment of malignancy.

In this paper we proposed a mathematical model for any kind of magnetic nanoparticles. Then by utilizing this model we can find the true location of tumor where nanoparticles are attaching themselves to it.

This paper consists of four sections. In section II a mathematical model has been proposed. In section III the detector system is studied and Results of Simulations of our model are presented in section IV, which approves our theoretical work.

Model of Magnetic Nanoparticles

Problem Statement

Spin and the related magnetic moment are primary properties of elementary particles. The spin quantum number relates to many phenomena in elementary particle physics as well as in nuclear and statistical physics. Spin is one type of angular momentum which does not have a classical analogy, but one may tentatively view a spin coming from a spinning motion of a nanoparticle. To this date, advancement in lithography and nanotechnology fabrication makes nanoparticles useful and feasible. In this case using of nanoparticles are needed a precise mathematical and physical model. To satisfy this demand we find a desirable model by utilizing Landau–Lifshitz Gilbert (LLG) equation. Then we perform this model to Received Signal Strength (RSS) localization system to find the location of nanoparticles. The received signals are coming from magnetic nanoparticles bound to "tumors". We aim to use this simulation study to reveal the theoretical possibility of magnetic nanoparticles for developing a low cost system capable of screening various types of cancers in a large population.

In magnetic nanoparticles, quantum mechanical effects become significant and Maxwell's equations alone will not be adequate to describe the behavior of magnetic materials. Obviously, simulating these nano-magnetic materials from a quantum physics point of view would give the most perfect description.

Due to have a mathematical model for magnetic nanoparticle we have utilized a semi-classical approach based on LLG equations [11]-[12] for nano scale materials.

The Bloch equation describes well the magnetization dynamics [13] of an ensemble of non-interacting or weakly interacting spins, but it does not capture the proper physics of a strongly interacting spin system such as a piece of magnet. This is because the magnetization magnitude of a magnet shall not change with time, and does not preserve the magnitude of the magnetization. To take into account the dissipative effect of the environment, we utilize LLG equations to describe our system instead of Bloch equations.

In our approach, we have used Finite Element Method (FEM) as a numerical technique for finding approximate solutions of partial differential equations (PDE). The solution approach is based either on steady state problems, or rendering the PDE into an approximating system of ordinary differential equations, which are then numerically integrated using standard techniques.

Landau–Lifshitz Gilbert Equations

Magnetization magnitude $|\mathbf{M}|$ for a specific material is constant and just dependant on environment temperature. The magnetization can be described as:

$$\mathbf{M} = |\mathbf{M}| \cdot \left(m_x \hat{i} + m_y \hat{j} + m_z \hat{k} \right) \tag{1}$$

Magnetic Gibbs free energy in nanoparticle (Etotal) consists of four elements: exchange energy, Zeemen energy, magnetostatic energy, and the anisotropy energy. These energies can be express as:

$$E_{exchange} = \frac{C}{2} \int (\nabla m_x)^2 + (\nabla m_y)^2 + (\nabla m_z)^2 \, dv \tag{2}$$

$$E_{magnetostatic} = \frac{\mu}{2} \int \mathbf{H_{in}} \cdot \mathbf{M} dv \tag{3}$$

$$E_{Zeemen} = \mu \int \mathbf{H}_{ex} \cdot \mathbf{M} dv \tag{4}$$

Where, C is exchange stiffness, and for nanoparticles is in order of 10-13(J/m) [14]. $\mathbf{H_{in}}$ is magnetic induction

for demagnetization field, $\mathbf{H}_{ex}$ is the magnetic induction vector of the externally applied field and μ is the permeability of free space. Furthermore there is also the anisotropy energy, which is intrinsic to the material. The most common form of anisotropy is the stress anisotropy. Crystalline anisotropy occurs due to the spin–orbit interaction of the electrons. Depending on their lattice structure, the magnetic materials have a preferred direction of magnetization. This is called the easy axis. Anisotropy energy can be described by [15]:

$$E_{anisotropy} = L_a \cdot V \cdot \sin^2(\beta) \quad (5)$$

Where β is the angle between the easy axis and the magnetization, L_a is the anisotropy constant, and V is the sample volume.

The dynamic of magnetic properties is governed by LLG equation:

$$(1+\alpha^2)\frac{d\mathbf{M}}{dt} = -\gamma\mathbf{M}\times\mathbf{H}_T - \alpha\gamma\mathbf{m}\times(\mathbf{M}\times\mathbf{H}_T) \quad (6)$$

Where γ is the gyromagnetic ratio (in order of 10^5), α is the damping constant and $\mathbf{H}_T$ is effective magnetic field:

$$\mathbf{H}_T = -\frac{\partial E_{totat}}{\partial M} \quad (7)$$

Solving LLG equation for nanoparticles is required 2D mesh generator because nano magnetic materials currently under investigation are magnetic thin films.

Thin films are really just a 2D structure where the thickness of the films is usually uniform.

We use a mesh generation algorithm which is based on a mechanical correlation between a triangular mesh and a 2D truss structure. In this algorithm any set of points in the x, y, z-plane (nanoparticles are in z=0) can be mapped onto the "natural coordinates" (ε, η, ξ) by the Delaunay algorithm [16]. In our proposed model the edges of Triangles (the connections between pairs of points) correspond to bars, and the points correspond to joints of the truss.

Each bar has a force-displacement relationship f(L,L0) depending on its current length L and its unextended length L_0 [16]. The magnitude of this force is just large enough to keep the node from moving outside. The positions of the joints (these positions are our principal unknowns) are found by solving for static force equilibrium in the desired structure. The hope is the lengths of all the bars at equilibrium will be nearly equal, giving a well-shaped triangular mesh.

We can solve force equilibrium in our structure by considering all (x,y,z)-coordinates in mesh points into an N-by-2 array Q=[x y z]. So the force equilibrium equation could be written:

$$F_q(Q) = \left[F_{ix}(Q) + F_{iy}(Q) + F_{iz}(Q)\right] + \left[F_{ex}(Q) + F_{ey}(Q) + F_{ez}(Q)\right] \quad (8)$$

Where Fi is the internal forces from the bars, and Fe is the external force (reactions from the boundaries). The Delaunay algorithm find out non overlapping triangles that fill the convex hull of the input points, such that every edge is shared by at most two triangles, and the circumcircle of every triangle contains no other input points [16].

For solving force equilibrium equation, we consider the system of ODEs:

$$\frac{dQ}{dt} = F(Q)$$
$$Q(0^+) = Q_{in} \quad (9)$$

The system is using forward Euler method for true approximation. The time is discretized by $t_n = n\Delta t$ and solution $Q_n = Q(t_n)$ is update by:

$$Q_{n+1} = Q_n + \Delta t F(Q_n) \quad (10)$$

There are some force functions that have been studied in [17-18]. The function k(L_0,L) models ordinary linear springs[17]. Our implementation uses this linear response for the repulsive forces but it allows no attractive forces:

$$f(L_0, L) = \begin{cases} k(L_0 - L) & L > L_0 \\ 0 & L < L_0 \end{cases} \quad (11)$$

If L_0 is chosen constant then it generates uniform meshes. However there are many cases when it is advantageous to have different sizes in different regions. Where the geometry is more complex, it needs to be resolved by small elements (geometrical adaptively). The solution method may require small elements close to a singularity to give good global accuracy (adaptive solver). A uniform mesh with these small elements would require too many nodes.

In our model we are using function H(x,y,z)as an element size to provide a desired edge length distribution. This function gives the relative distribution over the domain. So the number of node is not need to specify. In our implementation we use following function in MATLAB; function [Q,tri]=me_gen(G,L,h,B,fint,varargin).

Q is N-by-3 array contains the(x, y, z) coordinates for each of the N nodes. Size of N is important parameters for our model. The triangle indices tri. The row

associated with each triangle has 3 integer entries to specify node numbers in that triangle. G is a distance function which is given for the geometry. G returns the signed distance from each node location Q to the closest boundary.

The desired edge length function H(x, y, z) is given as a function L, which returns h(x,y,z) for all input points. The parameter h is the distance between points in the initial distribution Q_0. For uniform meshes, the element size in the final mesh will usually be a little larger than this input [16].

The bounding box for the region is an array B=[xmin, ymin; xmax, ymax] (the particle is in Z-plate). The fixed node positions are given as an array pfix with two columns. Additional parameters to the functions G and L can be given in the last arguments varargin. The variable varargin is a cell array containing the optional arguments to the function. It must be declared as the last input argument and collects all the inputs from that point onwards.

We will use directly with $d=\sqrt{\left(x^2+y^2+z^2\right)}-1$ which can be specified as an inline function. For a uniform mesh, h(x, y, z) returns a vector of 1's. The circle has bounding box $-1<x<1,-1<y<1, z=Z_0$, with no fixed points. A mesh with element size approximately h_0 = 0.2 is generated and the result is shown in Fig.1.

Any variable ϕ, Including the x, y, and z coordinates, can then be interpolated within the proposed mesh grid by:

$$\phi(\varepsilon,\eta,\zeta)=\sum_{i=1}^{88}N_i^e(\varepsilon,\eta,\zeta)\phi_i^e \tag{12}$$

And then Jacobian matrix for Eq. 12 is:

$$J=\begin{bmatrix}\sum_{i=1}^{88}\frac{\partial N_i}{\partial\varepsilon}x_i & \sum_{i=1}^{88}\frac{\partial N_i}{\partial\varepsilon}y_i & \sum_{i=1}^{88}\frac{\partial N_i}{\partial\varepsilon}z_i\\ \sum_{i=1}^{88}\frac{\partial N_i}{\partial\eta}x_i & \sum_{i=1}^{88}\frac{\partial N_i}{\partial\eta}y_i & \sum_{i=1}^{88}\frac{\partial N_i}{\partial\eta}z_i\\ \sum_{i=1}^{88}\frac{\partial N_i}{\partial\zeta}x_i & \sum_{i=1}^{88}\frac{\partial N_i}{\partial\zeta}y_i & \sum_{i=1}^{88}\frac{\partial N_i}{\partial\zeta}z_i\end{bmatrix} \tag{13}$$

Applying Eq.12 to Eq.1 gives:

$$\mathbf{M}=\left|M_S\right|\cdot\left(\sum_{i=1}^{88}N_i m_{xi}\tilde{i}+\sum_{i=1}^{88}N_i m_{yi}\tilde{j}+\sum_{i=1}^{88}N_i m_{zi}\tilde{k}\right) \tag{14}$$

Due to calculate the magnetic volume charge density we have:

$$\phi=-\frac{1}{4\pi}\int_V\frac{\nabla\cdot\left(\left|M_S\right|\cdot\left(\sum_{i=1}^{88}N_i m_{xi}\tilde{i}+\sum_{i=1}^{88}N_i m_{yi}\tilde{j}+\sum_{i=1}^{88}N_i m_{zi}\tilde{k}\right)\right)}{\left|\mathbf{r}-\mathbf{r}'\right|}dv' \tag{15}$$

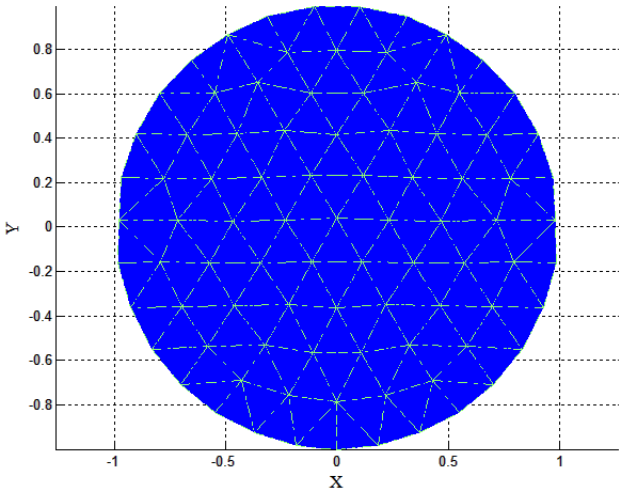

FIG. 1 AN UNIFORM MESH WITH ELEMENT SIZE OF 0.2. IN THIS MESH THE SIZE OF P IS 88.

And with some algebraic manipulation we have Eq. 16. Similarly, surface charge density is calculated by Eq. 17.

$$\phi_V=-\frac{\left|M_S\right|}{4\pi}\left\{\sum_{i=1}^{88}\frac{\left(\int_v\frac{dN_i}{dx}dv\right)m_{xi}+\left(\int_v\frac{dN_i}{dy}dv\right)m_{yi}+\left(\int_v\frac{dN_i}{dz}dv\right)m_{zi}}{\sqrt{\left(x_0-\sum_{j=1}^{88}N_j x_j\right)^2+\left(y_0-\sum_{j=1}^{88}N_j y_j\right)^2+\left(z_0-\sum_{j=1}^{88}N_j z_j\right)^2}}\right\} \tag{16}$$

$$\phi_S=-\frac{\left|M_S\right|}{4\pi}\left\{\sum_S\left[\sum_{i=1}^{88}\frac{\left(\int_S\frac{dN_i}{dx}ds\right)m_{xi}+\left(\int_S\frac{dN_i}{dy}ds\right)m_{yi}+\left(\int_S\frac{dN_i}{dz}ds\right)m_{zi}}{\sqrt{\left(x_0-\sum_{j=1}^{88}N_j x_j\right)^2+\left(y_0-\sum_{j=1}^{88}N_j y_j\right)^2+\left(z_0-\sum_{j=1}^{88}N_j z_j\right)^2}}\right]\right\} \tag{17}$$

For evaluating surface charge density, the unit normal vector should be calculated. Unit normal vector for any surface can be calculated by using Jacobian matrix.

$$\mathbf{N}(\varepsilon,\eta)=\frac{\partial(y,z)}{\partial(\varepsilon,\eta)}\mathbf{i}+\frac{\partial(x,z)}{\partial(\varepsilon,\eta)}\mathbf{j}+\frac{\partial(x,y)}{\partial(\varepsilon,\eta)}\mathbf{k} \tag{18}$$

The volume and surface charge terms are then summed for each element and then assembled into a global matrix just like any other finite element method:

$$\varphi_{total}=\varphi_V+\varphi_S \tag{19}$$

We have used interpolation functions as a weighting for Galerkin method. Then we multiply these weighting functions with LLG equation and integrate over the entire volume.

We then obtain the formulation of the LLG equation by using Green's theorem, which states that:

$$\sum_{j=1}^{88} W_{ij}\frac{dm_{xj}}{dt}=\frac{\gamma\mu}{1+\alpha^2}\Big(\frac{C}{|M|\mu}\sum_{j=1}^{88}\sum_{k=1}^{88}\int_v N_i\nabla N_j\cdot\nabla N_k dv.(m_{yj}m_{zk}-m_{zj}m_{yk})$$
$$+\sum_{j=1}^{88}\sum_{k=1}^{88}\phi_k(m_{yj}((\int_v(N_iN_j\nabla N_k dv)\cdot\mathbf{k})-m_{zj}((\int_v(N_iN_j\nabla N_k dv)\cdot\mathbf{j}))$$
$$-\sum_{j=1}^{88}\sum_{k=1}^{88}(\int_v N_iN_jN_k dv)(m_{yj}h_{zk}-m_{zj}h_{yk}))$$
$$+\frac{\gamma\mu\alpha}{1+\alpha^2}\Big(\frac{C}{|M|\mu}\Big(\sum_{j=1}^{88}\sum_{k=1}^{88}\sum_{l=1}^{88}\int_v(N_iN_j\nabla N_k\cdot\nabla N_l dv)(m_{yj}m_{xk}m_{yl}+m_{xj}m_{zxk}m_{zl}$$
$$+m_{xj}m_{zk}m_{zl}+m_{xj}m_{yk}m_{yl}+m_{zj}m_{xk}m_{zl}+2m_{xj}m_{xk}m_{xl})$$
$$+\sum_{j=1}^{88}\sum_{k=1}^{88}\sum_{l=1}^{88}\int_v(N_iN_j\nabla N_k\cdot\nabla N_l dv)(m_{xj}m_{zk}m_{zl}+m_{xj}m_{xk}m_{xl}+m_{xj}m_{yk}m_{yl}))$$
$$+\sum_{j=1}^{88}\sum_{k=1}^{88}\sum_{l=1}^{88}m_{yj}m_{xk}((\int_v(N_iN_jN_k\nabla N_l dv)\cdot\mathbf{j})\phi_1-(\int_v N_iN_jN_kN_l dv)h_{yl})$$
$$+\sum_{j=1}^{88}\sum_{k=1}^{88}\sum_{l=1}^{88}m_{xj}m_{zk}((\int_v(N_iN_jN_k\nabla N_l dv)\cdot\mathbf{k})\phi_1-(\int_v N_iN_jN_kN_l dv)h_{zl})$$
$$+\sum_{j=1}^{88}\sum_{k=1}^{88}\sum_{l=1}^{88}m_{xj}m_{xk}((\int_v(N_iN_jN_k\nabla N_l dv)\cdot\mathbf{i})\phi_1-(\int_v N_iN_jN_kN_l dv)h_{xl})$$
$$-\sum_{j=1}^{88}((((\int_v(N_i\nabla N_j dv)\cdot\mathbf{i})-(\int_v N_iN_j dv)h_{xj})) \quad (20)$$

Where;

$$W_{ij}=\int_v N_iN_j dv \quad (21)$$

In matrix term Eq. 20 is expressed as:

$$W_{ij}F_j(m_j)=G_i \quad (22)$$

$F(m_x)$ is the derivative of m_x with respect to time G_i is the combined terms on the left hand side of Eq. 20. W_{ij} is the coefficient for $F(m_x)$ and it is a symmetrical matrix. We have been solved Eq. 22 by using time stepped integration and the fourth order Runge–Kutta formula [17]. In This method (m_x, m_y, m_z) should be normalized at the end of every time step iteration to guarantee: $\left|m_x\hat{i}+m_y\hat{j}+m_z\hat{k}\right|=1$

In Eq. 22 W_{ij} is 88×88 matrix, and MATLAB cope with this kind of large matrix proficiently using the function sparse. Using the function sparse speed up the matrix inversion calculation and will make the whole system is a real time system.

The global matrix for the FEM is assembled from these elemental matrices in the usual way. We use fourth-order Runge Kutta formula [18] to advance the solution from m^n to m^{n+1}.

$$m^{n+1}=m^n+\frac{k_1}{6}+\frac{k_2}{3}+\frac{k_3}{3}+\frac{k_4}{6} \quad (23)$$

Where:

$$k_1=(timestep)F(m^n)$$
$$k_2=(timestep)F(m^n+\frac{k_1}{2})$$
$$k_3=(timestep)F(m^n+\frac{k_2}{2})$$
$$k_4=(timestep)F(m^n+k_3)$$

In our simulation a time step on the order of 1 fs is usually provided a good accuracy.

In Runge Kutta formula, the easiest way to stop the step time iteration is to terminate when the rate of change of the magnetization component is less than 0.01° per fs. If the time step is in fs, then this rate of change is given by:

$$\frac{d\theta}{dt}=\cos^{-1}\Big(\frac{\mathbf{m^n}\cdot\mathbf{m^{n+1}}}{|\mathbf{m^n}\cdot\mathbf{m^{n+1}}|}\Big)\times\frac{180}{\pi\times timestep}<0.01^\circ \quad (24)$$

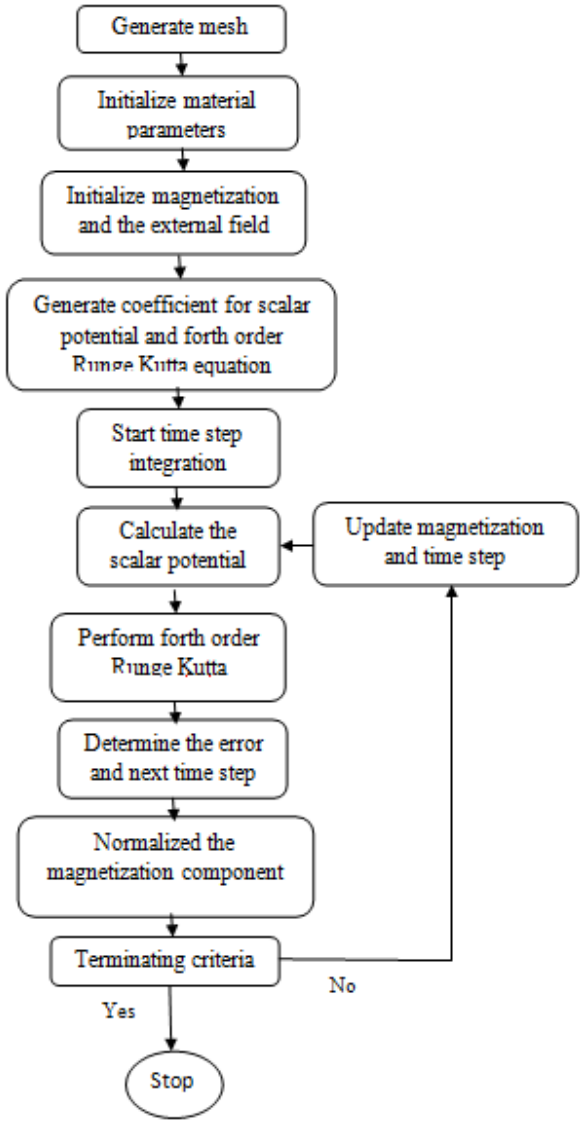

FIG. 2 THE FLEWCHART OF PROPOSED MODEL

The described algorithm has been illustrated in details in FIG. 2.

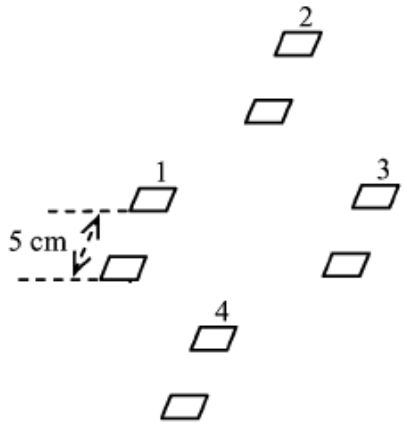

FIG. 3 THE DETECTOR SYSTEM INCLUDING 4 SQUIDs

Detector System

Our detection system is containing four gradient coils of SQUIDs (gradiometers) [19] marked by numbers 1 through 4 (FIG. 3).

The SQUIDs are used to detect and measure the signals which are produced by magnetic nanoparticles. They have a capability to detect vary small magnetic fields due to the high sensitivity [20].

Commercial Magneto-Encephalo-Graphic (MEG) systems, which are usually equipped with several hundreds of SQUID channels, are increasingly available in clinical settings. These systems are capable of measuring extremely weak magnetic fields on the order of 10-14T produced by active groups of neurons within the brain[20].

Applying the measured signals to the proposed algorithm four distances can be achieved. Here Di is indicated the distance between i-th coil and magnetic nanoparticles. The magnetic field signal from the tumor (magnetic nanoparticles) is calculated at the central point of the two coils. The spacing between each pair of the gradient coils is 5 cm wide and 0.75 cm high.

The detection system provides four distance [D_1 D_2 D_3 D_4]. Using RSS localization, the location of tumor can be identified precisely.

Simulation and Result

Our study utilized three types of magnetic nanoparticles manufactured by Chemicell GmbH in Germany as listed in table 1.

The particles from Chemicell GmbH were supplied in the form of ferrofluid with dispersion of magnetic nanoparticles (iron oxides). These particles are coated with hydrophilic polymer matrices that prevent them from being aggregated by foreign ions. Using terminal functional groups of agents such as ion-exchange group or reactive group for covalent immobilization, these ferrofluids can bind to biological molecules as biomarkers for a number of applications such as MRI-based diagnosis and targeted drug delivery.

TABLE 1 THREE KIND OF NANOPARTICLES USING IN THIS PAPER

Product name	Core	Size (nm)	Polymer matrix
FluidMAG-DXS	Fe_3O_4	100	Dextran sulfate
FluidMAG-CMX	Fe_3O_4	250	Polyethylenimine
FluidMAG-PEI	Fe_2O_3	250	Carboxymethyl dextran

Magnetic field simulation:

In this simulation we are applying the proposed algorithm which is illustrated in FIG. 2 over three magnetic nanoparticles. Then the simulation result of the algorithm is compared to our experimental data. The experimental data is achieved by using the 306-channel Elekta Neuromags MEG system manufactured by Elekta Neuromag Oy (Helsinki, Finland).

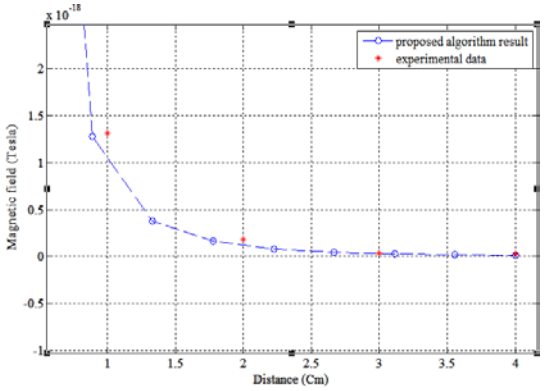

FIG. 4 SIMULATING FluidMAG-PEI WITH 1.212 DAMPING CONSTANT

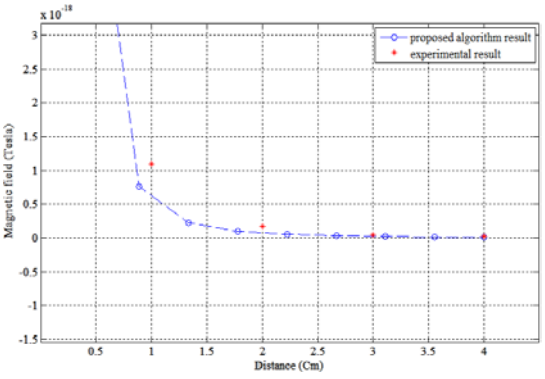

FIG. 5 SIMULATING FluidMAG-CMX WITH 0.932 DAMPING CONSTANT

Tumor localization:

In order to simulate the RSS localization based on the proposed algorithm we have utilized a simplified human model as shown in FIG. 7.

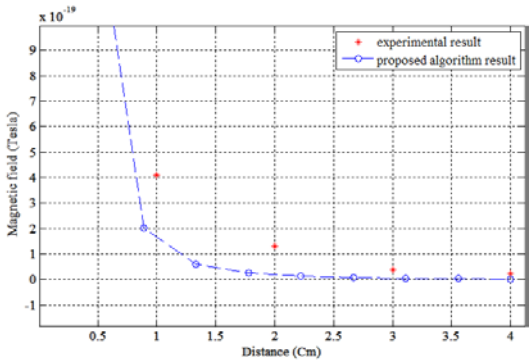

FIG. 6 SIMULATING FluidMAG-DXS WITH 0.932 DAMPING CONSTANT

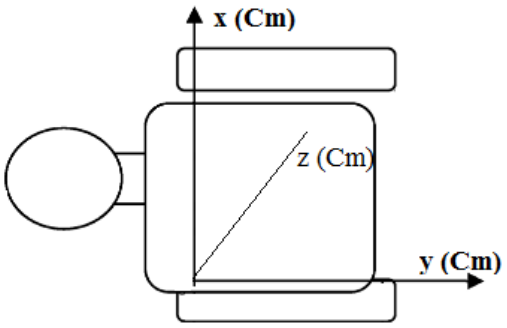

FIG. 7 A SIMPLIFIED MODEL FOR HUMAN BODY

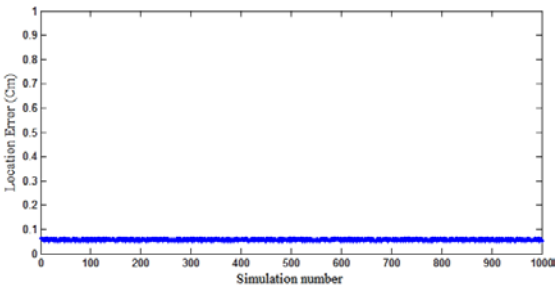

FIG. 8 LOCALIZATION ERROR OVRE 1000 TEST USING FluidMAG-PEI

Conclusion

In this paper, we have studied a tumor localization system based on magnetic nanoparticles. The proposed system is consisting of four gradiometers. The SQUIDs which act as detectors sense the signals produced by the magnetic nanoparticles attached to tumors. We have proposed mathematical model for magnetic nanoparticles based on LLG equations. In this system nanoparticles act as a signal sources in the human body and four SQUIDs act as base station that find the true location of nanoparticles.

Our simulation has provided estimates of the system sensitivity for tumors located at different sites of the body. The results of simulation prove that the location error in 1000 test is less than 0.1 Cm is around 0.08Cm.

Our results have shown that, by combining nanotechnology with SQUIDs, tumors can be detected. Using this new method, it is possible to detect tumors at early stages containing only hundreds of cancerous cells. Once this system is developed, it may be used to scan a large number of people rapidly to detect various types of cancers at different body locations. The actual design and construction of this system as well as the tumor localization will be our next steps of investigation.

REFERENCES

Hartman, K. B., Wilson, L. J., and Rosenblum, M. G. (2008) Detecting and treating cancer with nanotechnology. *Mol Diagn Ther* **12**(1), 1–14.

Cuenca, A. G., Jiang, H., Hochwald, S. N., Delano, M., Cance, W. G., and Grobmyer, S. R. (2006) Emerging implications of nanotechnology on cancer diagnostics and therapeutics. *Cancer* **107**(3), 459–466.

Alexis, F., Rhee, J. W., Richie, J. P., Radovic-Moreno, A. F., Langer, R., and Farokhzad, O. C. (2008) New frontiers in nanotechnology for cancer treatment. *Urol Oncol* **26**(1), 74–85.

De Jong, W. H. and Borm, P. J. (2008) Drug delivery and nanoparticles: applications and hazards. *Int J Nanomedicine* **3**(2), 133–149.

Duncan, R., Kreyling, W. G., Biosseau, P., Cannistraro, S., Coatrieux, J., Conde, J. P., Hennick, W., Oberleithner, H., and Rivas, J. (2005) ESF scientific forward look on nanomedicine. In European Science Foundation Policy Briefing. 1–6.

Cho, K., Wang, X., Nie, S., Chen, Z. G., andShin, D. M. (2008) Therapeutic nanoparticles for drug delivery in cancer. *Clin Cancer Res* **14**(5), 1310–1316.

Jun, Y. W., Jang, J. T., and Cheon, J. (2007) Magnetic nanoparticle assisted molecular MR imaging. *Adv Exp Med Biol* **620**, 85–106.

Will, O., Purkayastha, S., Chan, C., Athanasiou, T., Darzi, A. W., Gedroyc, W., and Tekkis, P. P. (2006) Diagnostic precision of nanoparticle-enhanced MRI for lymph-node metastases: a meta-analysis. *Lancet Oncol* 7(1), 52–60.

Study on the Feasibility to Detect Cancer Tumors by Combining Nanotechnology With SQUID

Nanotechnology for Genomic Signal Processing in Cancer Research

W.F. Brown, *Micromagnetics*, Interscience Publishers, New York, 1963.

W. Brown Jr., Domains, micromagnetics, and beyond: Reminiscences and assessments, *J. Appl. Phys*. 49, 1937–1942, 1978.

X. R. Wang, Y. S. Zheng, and S. Yin, *Phys. Rev. B* **72**, R121303 (2005).

M. Klaui and C.A.F. Vaz, Magnetization configurations and reversal in small magnetic elements, *Handbook of Magnetism and Advanced Magnetic Materials*, HKronmüller and S. Parkin, Eds., John Wiley & Sons, Chichester, U.K., 2007.

J. Fidler, R.W. Chantrell, T. Schrefl, and M. Wongsam, Micromagnetics I: Basic principles, in *Encyclopedia of Materials: Science and Technology*, K.H.J. Buschow, R.W. Cahn, M.C. Flemings, B. Ilschner, E.J. Kramer, and S. Mahajan, Eds., Elsevier Science Ltd, Oxford, England, 2001, pp. 5642–5651.

H. Edelsbrunner, Geometry and Topology for Mesh Generation, Cambridge University Press,2001.

K. Shimada and D. C. Gossard, Bubble mesh: automated triangular meshing of non-manifold geometry by sphere packing, in SMA '95: Proceedings of the Third Symposium on Solid Modeling and Applications, 1995, pp. 409–419.

W.H. Press, B.P. Flannery, S.A. Teukolsky, andW.T. Vetterling, *Numerical Recipes in C: The Art of Scientific Computing*, 2nd ed. Cambridge University Press, 1992.

K. Enpuku, K. Inoue, and K. Soejima *et al.*, "Magnetic immunoassays utilizing magnetic markers and a high-Tc SQUID," *IEEE Trans. Appl. Supercond.*, vol. 15, pp. 660–663, 2005.

E.R. Flynn, H.C. Bryant, Phys. Med. Biol. 50 (2005) 1273.